ELSEVIER

Thermochimica Acta 374 (2001) 13–22

thermochimica acta

www.elsevier.com/locate/tca

The effect of temperature on the properties of hydroxyapatite precipitated from calcium hydroxide and phosphoric acid

Slavica Lazić[1], Slavica Zec, Nada Miljević, Slobodan Milonjić*

The Vinča Institute of Nuclear Sciences, P.O. Box 522, 11001 Belgrade, Yugoslavia

Received 15 December 2000; accepted 16 January 2001

Abstract

The effect of temperature on stoichiometry, morphology and crystallinity of hydroxyapatite (HA) prepared from calcium hydroxide and phosphoric acid was investigated.

The crystals precipitated in the temperature range 22–95°C and matured for 20 h at precipitation temperature have shown the properties of thermally stable HA. The size and crystallinity of the crystals increase with an increase of the preparation temperature.

HA precipitated at 95°C shows thermal stability even without ripening. The importance of the maturation stage in obtaining thermally stable HA increases with decreasing precipitation temperature.

HA precipitated at low temperature (22°C) after appropriate maturation shows the properties of stoichiometric low crystalline HA and appears to be very promising as a bioceramic precursor.

Keywords: Hydroxyapatite; Crystallization; Biomaterials; Stoichiometry; Thermal stability

1. Introduction

Hydroxyapatite (HA), $Ca_{10}(PO_4)(OH)_2$, is a compound of great interest in different fields. As a compound with structural and chemical resemblance of bone mineral, HA is of particular importance in the field of biomaterials. The properties that make HA superior as a biomaterial are absence of toxicity and high compatibility with hard and soft tissues [1–3].

While numerous applications of HA were reported and various preparation methods have been used [4–6], powder and slurry still present most important raw material forms. Some major applications include:

1. surface coating of orthopedic and dental metal implants, with plasma spraying as a most commonly used method [7–10]. The role of HA coating is two-fold: promoting osseointegration process (bone tissue formation at implant surface) and reducing metal ions release by acting as a physical barrier;
2. bioceramics preparation, for the purpose of replacement of fragments of weight-unloaded bones, repair of periodontal bony defects, ridge augmentation, ear implants, etc. [1,11];
3. drug carrier for controlled drug release based on adsorption/desorption properties of bioactive molecules (growth hormone, antibiotics) with

---

*Corresponding author. Tel.: +381-11-444-0871; fax: +381-11-444-5472.

E-mail addresses: slazic@netscape.net (S. Lazić), smiloni@rt270.vin.bg.ac.yu (S. Milonjić).

[1] Present address: 66 Pacific Avenue, Suite 811, Toronta, Ont., Canada M6P 2P4.

PII: S0040-6031(01)00453-1

promising potential to heal bone fractions and/or suppress inflammation process [2,12–14].

Different techniques have been used for HA powders preparation [15–21]. Depending upon the technique, materials with various morphology, stoichiometry, and level of crystallinity have been obtained. These properties essentially affect quality of biomaterials through the effects of phase thermal stability, mechanical integrity, and dissolution behavior.

Sintering of pure stoichiometric HA powder yields pure dense HA ceramics with superior mechanical properties, while during sintering of nonstoichiometric HA other phases are formed: CaO if Ca/P molar ratio exceeds 1.67 and TCP if Ca/P is below 1.67 [8,10,16,19].

The changes in bioceramics composition decrease strength of the material, increase its dissolution, and consequently affect the rate and extent of biodegradation.

Morphology and size of HA crystals have important role in bioceramics sintering [16,18,19]. Superior mechanical properties are obtained when stoichiometric HA with small and uniform crystal size is used as a precursor. On the other hand, sintering of well-crystallized HA yields less dense ceramics, mainly due to the voids in secondary aggregates that gather up during sintering.

Technological properties are governed by crystalline structure in many other advanced HA applications. In pharmaceutical use of HA as a drug excipient, compression ability is chiefly affected by the composition and crystal size [20]. In HA application, as a plastic stabilizer, e.g. styrene suspension polymerization, nonadequate stoichiometry and particle size was proven to be the main cause of the process failure, e.g. [21].

From the point of view of raw materials preparation, tailoring properties towards obtaining low crystalline HA with thermally stable composition appears to be the most promising direction [22].

When precipitation as a preparation method is applied, major parameters that should be taken into account include temperature, reagents concentration, addition rate, stirring, maturation, and presence of impurities.

In [23], a method for the obtaining stoichiometric apatite from calcium hydroxide and phosphoric acid was described, and HA crystals with theoretical lattice parameters were obtained. It was shown that crystal growth is almost completed during first 20 h maturation at 95°C. Further aging in aqueous solution contributes to crystal structural perfection, but the effect on HA stoichiometry and crystal size, the properties most relevant for material technological performance, is not significant.

Crystals obtained by described method are relatively large (specific surface area, 22 $m^2 g^{-1}$) which may cause porosity of sintered forms. In this paper, the effects of maturation time and temperature were investigated in order to optimize the procedure with respect to thermal stability of the composition and find compromise between crystal size and stoichiometry.

2. Experimental

2.1. Preparation method

HA was prepared from alkaline aqueous solutions by slow titration method in inert atmosphere, as it was described in [23]. The reagents were introduced at molar ratio Ca/P = 1.66. The $Ca(OH)_2$ suspension was prepared by slurring CaO powder ($CaCO_3$, Merck, analytical grade, calcinated for 24 h at 1000°C) into freshly double distilled water (DDW). Reagent grade H_3PO_4 was purified by crystallization method and reagent solution was prepared.

About 500 ml of $Ca(OH)_2$ suspension was placed in a thermostated reaction vessel, stirred intensively, and titrated with 0.5 M H_3PO_4 at a rate of 1 ml min^{-1}. Precipitation temperature was in the range 22–95°C.

The course of reaction was followed by pH measuring (Radiometer pH electrode GK 2401 B was used). After titration had been completed, some of the samples were further matured at precipitation temperature for 20 h. During maturation, the samples were intensively stirred. The sample HA11A, prepared under the same conditions as the sample 10, was matured without stirring. After preparation, supernatant was siphoned off and crystals were washed with DDW three times.

2.2. Characterization of the powders

HA crystals were identified by the X-ray diffractograms (XRD) and IR spectra. HA stoichiometry was determined from XRD of the samples annealed at 900°C for 2 h, based on phase thermal stability criteria [24]. X-ray analysis was performed by Siemens Model D 500 diffraction system using Cu Kα radiation. Lattice parameters of HA crystals were calculated from 4 1 0, 3 0 0, 0 0 4 and 0 0 2 diffraction peaks. Crystallite size was obtained from broadening of the 0 0 2, 2 2 2, and 3 0 0 diffraction peaks using Scherrer equation.

Purity of the samples was tested by IR spectral analysis. IR transmittance spectra of the ground samples were obtained in the 4000–400 cm^{-1} region on Specord 75 IR, Carl Zeiss by using KBr pellet technique (0.1 wt.%). The blank KBr pellet was placed in the reference beam. The weight loss and thermal stability of the samples were also evaluated from the thermogravimetric analysis data. A Stanton microbalance with a heating rate of 10° min^{-1} was employed.

The morphology of the solid particles was analyzed by transmission electron microscopy (TEM) using a Philips TEM 300 microscope. The samples were treated by ultrasound prior TEM observation in order to split the aggregates. Crystal size was estimated from TEM micrographs. About 100 crystals per sample were measured.

The specific surface area of the synthesized samples, degasified at 200°C was determined by nitrogen sorption/desorption according to single point BET method. Srohlein areameter was employed.

3. Results and discussion

Precipitation conditions and related properties of the crystals are shown in Table 1.

Stoichiometry of the samples was evaluated according to the reactions characteristic for thermal decomposition of nonstoichiometric HA at annealing temperature. Although lower than sintering temperature (usual range 1100–1200°C), this temperature is most characteristic with respect to HA stoichiometry and corresponding bioceramics composition.

Decomposition of calcium deficient apatites ($Ca/P < 1.67$) in the temperature range 22–900°C takes place according to the reaction

$$\mathrm{Ca_{10-\mathit{x}}(HPO_4)(PO_4)_{6-\mathit{x}}(OH)_{2-\mathit{x}}} \rightarrow x\mathrm{Ca_9(PO_4)_6}(\beta) + (1-x)\mathrm{Ca_{10}(PO_4)_6(OH)_2} \quad (1)$$

while in the samples with excess of $Ca(OH)_2$ during thermal treatment CaO is formed.

At higher temperatures (1200°C) further decomposition may occur according to the reaction presented by Eq. (2). The extent of the reaction is very much dependent on initial stoichiometry of HA. Ca deficient HA shows high degradation tendency, while in the case of stoichiometric HA some loss of OH^- groups takes place [24].

$$\mathrm{Ca_{10}(PO_4)_6(OH)_2} \rightarrow 2\mathrm{Ca_3(PO_4)_2}(\alpha) + \mathrm{Ca_4P_2O_9} + \mathrm{H_2O} \quad (2)$$

Formed compounds are proven to be the cause of coating and ceramics cracking due to related dissolution reactions under physiological conditions

$$3\mathrm{Ca_4P_2O_9} + 3\mathrm{H_2O} \rightarrow \mathrm{Ca_{10}(PO_4)_6(OH)_2} + 2\mathrm{Ca^{2+}} + 4\mathrm{OH^-} \quad (3)$$

Table 1
The effect of the precipitation conditions on crystal size and lattice parameters of hydroxyapatite crystals

Precipitation conditions				Crystallite size (nm)			Surface area ($m^2 g^{-1}$)		Lattice parameters (nm)	
Sample	Temperature (°C)	pH	Maturation time (h)	L_{002}	L_{300}	L_{222}	Sm	Sc	*a*	*c*
HA6	95	10.60	0	58	38	46	36	30	0.9420	0.6895
HA7	95	10.60	20	79	56	62	23	23	0.9419	0.6887
HA8	70	11.63	20	69	39	42	34	28	0.9418	0.6894
HA9	70	11.63	0	43	27	27	40	42	0.9406	0.6888
HA10	22	12.80	20, stirring	26	–	18	58	–	0.9393	0.6861
HA11	22	12.80	0	55	18	24	46	52	0.9438	0.6884
HA11A	22	12.80	20, no stirring	49	18	23	53	54	0.9427	0.6874

and

$$4\mathrm{Ca_3(PO_4)_2} + 2\mathrm{H_2O} \rightarrow \mathrm{Ca_{10}(PO_4)_6(OH)_2} + 2\mathrm{HPO_4}^{2-} + 2\mathrm{Ca}^{2+} \qquad (4)$$

3.1. XRD results

XRD spectra of all the samples, analyzed as-prepared, have shown peaks characteristic for HA. The crystals precipitated by the described method in the investigated temperature range and matured for 20 h at precipitation temperature have the properties of stoichiometric HA. No other phases were detected on the XRD of the samples annealed at 900°C for 2 h. Lattice parameters of the crystals precipitated and matured at 95°C were very close to the theoretical values (0.6884 and 0.9418 nm) [25].

Stoichiometry of the nonmatured samples varied significantly with temperature of preparation. The sample precipitated at 95°C shows properties of thermally stable stoichiometric HA. In the samples precipitated at lower temperatures, other phases were detected after annealing at 900°C: the presence of 3–4 wt.% of CaO was detected in the sample precipitated at 70°C, while HA precipitated at lower temperatures (22°C) decomposed into the mixture of HA and TCP (Table 2).

In the case of low temperature precipitation, stirring in the maturation stage has shown essential role in obtaining required stoichiometry. The sample matured without stirring decomposed into mixture of HA and TCP (sample HA11A), while the sample obtained by maturation under conditions of vigorous stirring shows the characteristics of thermally stable HA (sample HA10).

Table 2
Properties of the samples after annealing at 900°C

Sample	Phase composition and crystallite size (nm)			
	Phases	L_{002}	L_{300}	L_{222}
HA6	HA	96	77	72
HA7	HA	96	73	79
HA8	HA	85	67	78
HA9	HA, CaO (3–4%)	109	68	77
HA10	HA	79	65	81
HA11	HA + TCP	–	–	–
HA11A	HA + TCP	–	–	–

Characteristic diffractograms are presented in Fig. 1.

The size of individual HA crystals was calculated from broadening 0 0 2, 2 2 2, and 3 0 0 diffraction peaks, assuming that HA crystals were prisms with height equal to crystallite size along 0 0 2 plane and length of prism corresponding to crystallite size along 3 0 0 plane (Table 1). During annealing, crystallites show nonuniform growth and obtain more spherical form.

3.2. IR results

Recorded IR spectra of the samples have shown bands characteristic for HA. The bands at 3572 and 631 cm^{-1} are characteristic for stretching and librational modes of the OH^- ions, respectively. Characteristic frequencies derived from $\mathrm{PO_4}^{3-}$ modes can be seen at 1092, 1040, 962, 601, 571, and 474 cm^{-1} [26]. The IR peak at 875 cm^{-1} characteristic for $\mathrm{HPO_4}^{2-}$ was observed at the samples HA11 and HA11A. There was no noticeable $\mathrm{CO_3}$ absorption at 1410 cm^{-1} except for the sample HA10 (probably contaminated by the $\mathrm{CO_2}$ absorption from the air during sample handling). The IR spectra of the samples are shown in Fig. 2.

3.3. TGA results

The results of thermal analysis are shown in Fig. 3.

In the investigated temperature range there are three regions of interest:

1. up to 200°C, corresponding to the removal of adsorbed water;
2. between 200 and 650°C, corresponding to $\mathrm{HPO_4}^{2-}$ decomposition according to the reaction $2\mathrm{HPO_4}^{2-} \rightarrow \mathrm{P_2O_7}^{4-} + \mathrm{H_2O}$. Removal of interstitial water may also take place in this temperature range [27];
3. in the range 700–850°C, reaction $\mathrm{P_2O_7}^{4-} + 2\mathrm{OH}^- \rightarrow 2\mathrm{PO_4}^{3-} + \mathrm{H_2O}$ may take place.

The content of adsorbed water in the analyzed samples was in the range 2–2.52 wt.%, and total weight loss was between 4 and 6.5 wt.%, depending on crystallinity and stoichiometry of the samples. Except for the samples HA11 and HA11A weight loss in the range 700–850°C was small comparing with the loss measured at lower temperatures and can be ascribed to the removal of interstitial water rather than to thermal decomposition of the samples. This conclusion is corroborated with the IR and XRD results.

3.4. Morphology and size of crystals

Precipitation conditions have shown significant effect on crystal size and morphology. The crystals precipitated at 22°C have the form of tiny needles with average length of 110 nm and width of 11 nm. Maturation under conditions of precipitation does not

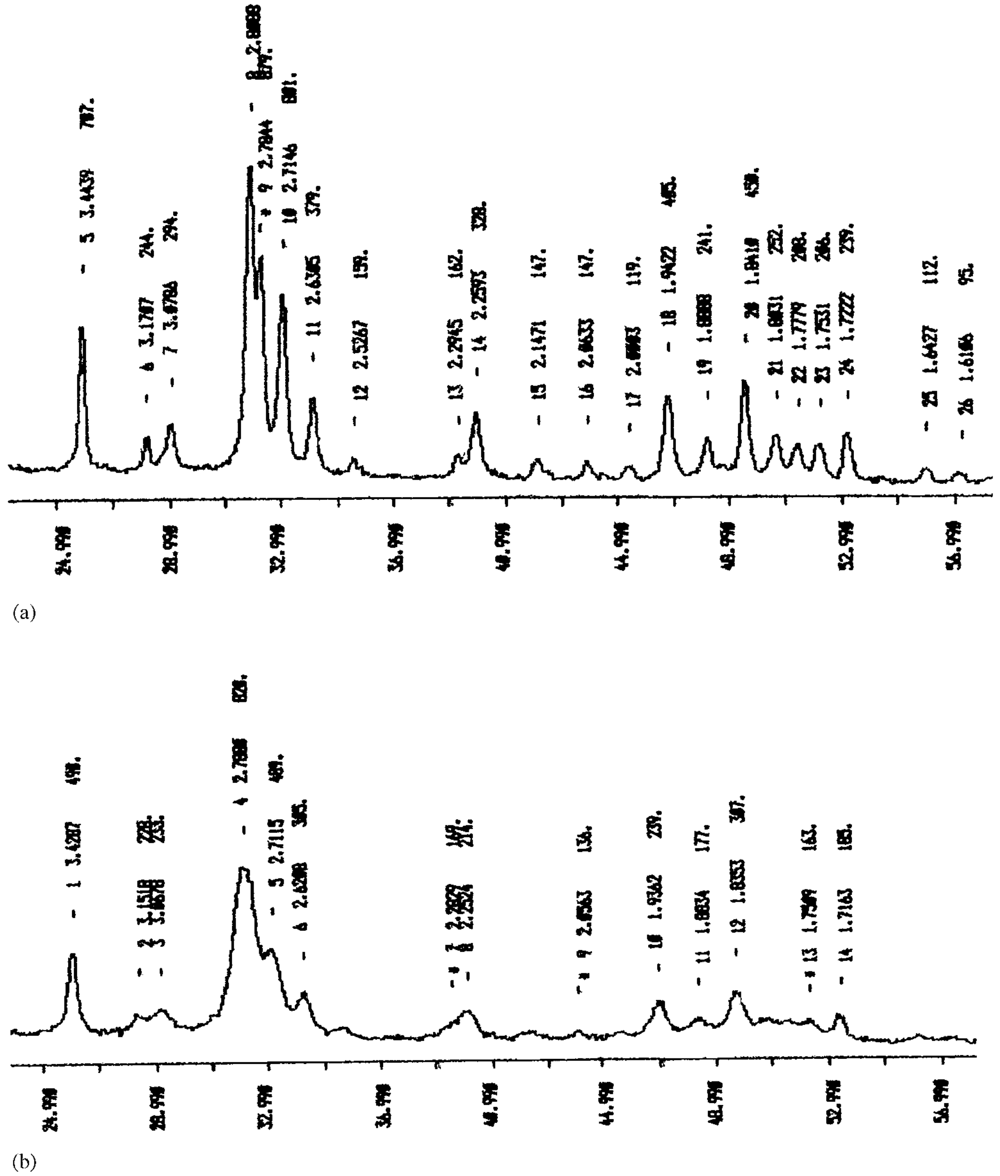

(a)

(b)

Fig. 1. X-ray diffractograms of the samples. (a) HA9; (b) HA10; (c) HA9 annealed at 900°C for 2 h; (d) HA10 annealed at 900°C for 2 h.

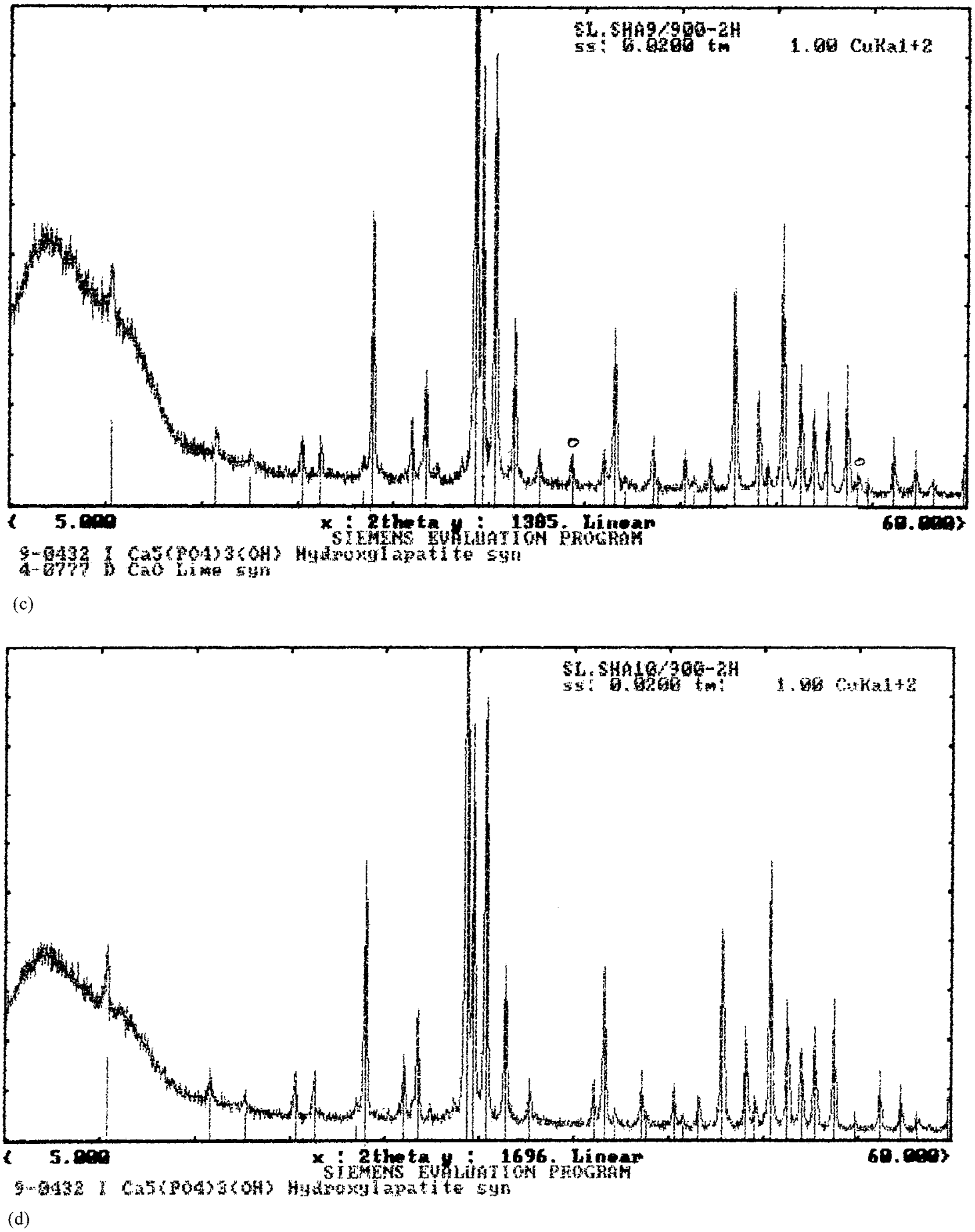

Fig. 1. (*Continued*).

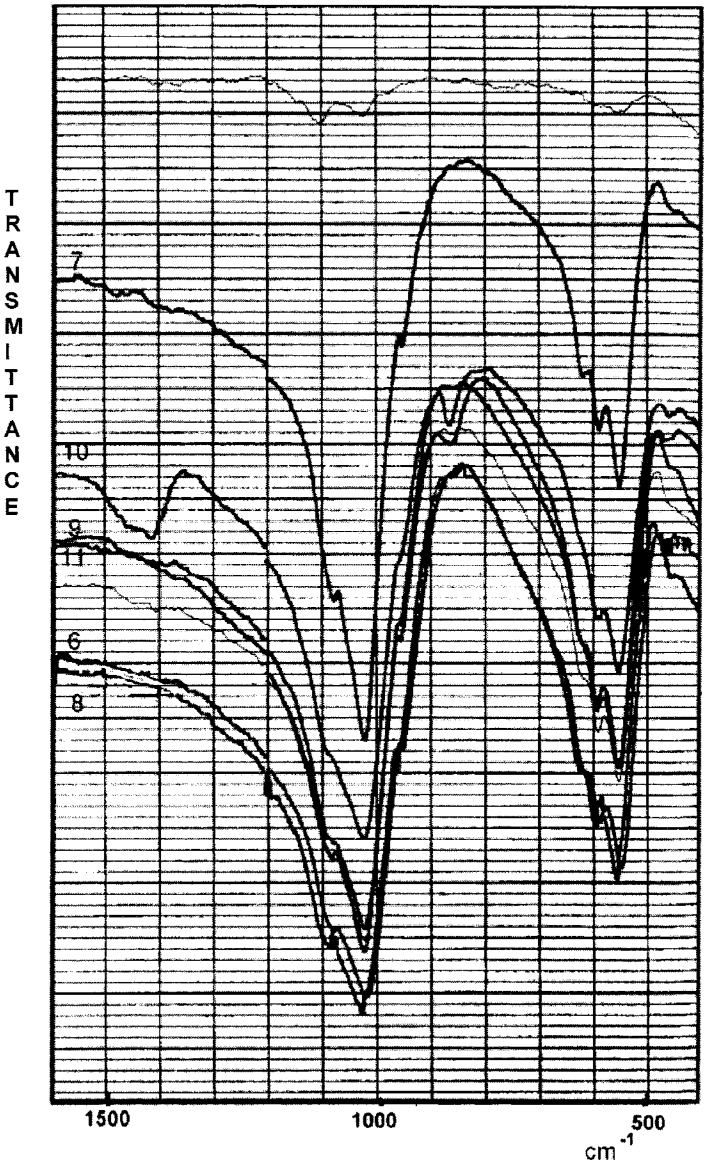

Fig. 2. IR spectra of the samples.

significantly affect crystal size. The crystals however become thicker and aggregation more pronounced.

Crystals precipitated at high temperature are well-rounded.

Average width of the crystals prepared at 70°C was in the range 11–33 nm (about 40% of measured crystals had width of 33 nm) and crystal length was between 55 and 200 nm.

Crystals formed at 95°C have length of 55–220 nm and width of 33–110 nm (30% of measured crystals had 55 nm width). Characteristic TEM micrographs are shown in Fig. 4.

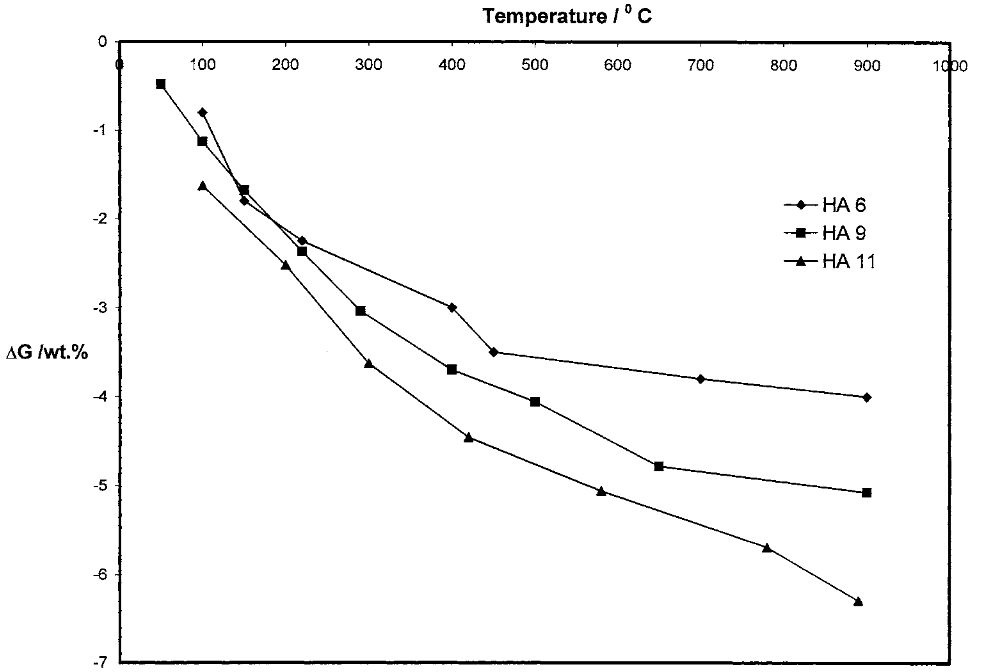

Fig. 3. TGA of the characteristic hydroxyapatite samples.

Based on the observation of TEM micrographs of the samples, larger width of crystals can be explained by crystals bonding, which predominantly takes place along *a–c* side. The smaller length of crystals can be attributed to the crystals ordering.

Specific surface area of the crystals (Sp) was in the range 23–58 $m^2\,g^{-1}$ and shows decrease with an increase of precipitation temperature and maturation time. Excellent agreement between measured values and those calculated from the broadening of XRD peaks was obtained for the sample precipitated and matured at 95°C, while for the samples prepared at lower temperatures deviation was in the range 5–15%.

4. Conclusions

Obtained results have shown that stoichiometry, size, morphology, and ordering of HA crystals precipitated from calcium hydroxide and phosphoric acid are significantly affected by the temperature and maturation conditions.

The crystals precipitated in the temperature range 22–95°C and matured for 20 h at precipitation conditions show the properties of thermally stable HA.

The crystals precipitated at 95°C show thermal stability even without further ripening. The importance of the maturation stage in obtaining stoichiometric HA increases with decreasing precipitation temperature.

Crystal ordering increases with an increase of preparation temperature. Nearly theoretical values for lattice parameters were obtained for the sample precipitated and matured at 95°C.

Crystal size increases with an increase of preparation temperature. Specific surface area of the crystals was in the range 23–58 $m^2\,g^{-1}$.

The crystals obtained at low temperature have form of tiny needles with uniform size (length of 110 nm and width of 11 nm). Length and width of the crystals increase with preparation temperature. Crystals formed at 95°C have length of 55–220 nm and width of 33–110 nm.

The effect of temperature in the early stages of crystal formation can be attributed to the lower supersaturation (due to lower $Ca(OH)_2$ solubility). In the maturation stage, apart from enhancing crystal structural ordering, increase of temperature brought about pronounced crystal aggregation and bonding.

Obtained results present good basis for tailoring HA properties in desirable direction that can be exploited in biomaterials preparation and other fields of HA application.

HA crystals precipitated at low temperature with small and uniform size, and thermally stable composition, appear very promising as a bioceramic precursor. However, due to low crystallinity, these crystals are very susceptible to the effects of stirring and chemical media, and maturation conditions have crucial role in obtaining required stoichiometry.

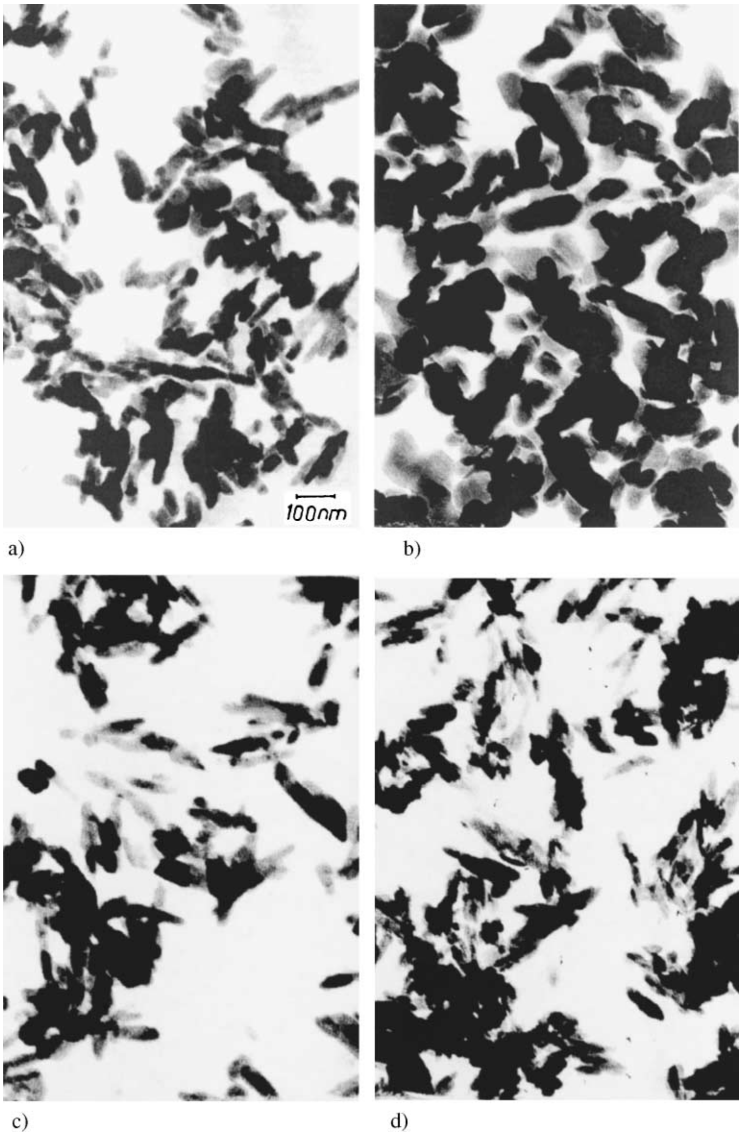

a) b) c) d)

Fig. 4. TEM micrographs of the characteristic samples. (a) HA6; (b) HA7; (c) HA8; (d) HA9; (e) HA10; (f) HA11. Magnification, 90,000×.

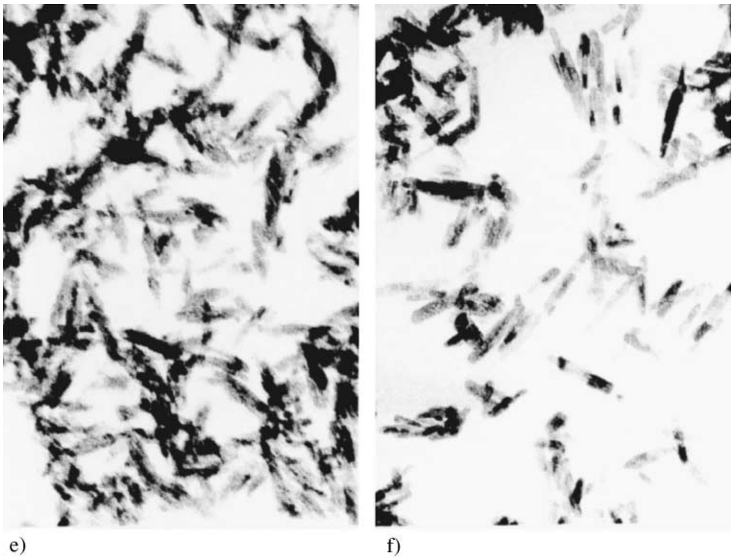

Fig. 4. (*Continued*).

References

[1] R.Z. LeGeros, Calcium Phosphates in Oral Biology and Medicine, Monographs in Oral Science, Vol. 15, Karger, Basel, 1991.

[2] H. Aoki, Science and Medical Applications of Hydroxyapatite, Japanese Association of Apatite Science (JAAS), Tokyo, 1991.

[3] W. Suchanek, M. Yoshimura, J. Mater. Res. 13 (1998) 94.

[4] P. Ducheyne, MRS Bull. 23 (1998) 43.

[5] R.P. Rusin, G.S. Fishman (Eds.), Bioceramics: Materials and Applications. II. Ceramic Transactions, Vol. 48, The American Ceramic Society, Westerville, 1996.

[6] D. Muster (Ed.), Biomaterials, Hard Tissue Repair and Replacement, European Materials Research Society Monographs, Vol. 3, Elsevier, Amsterdam, 1992.

[7] K.A. Khr, Y. Wang, P. Cheang, Surf. Eng. 14 (1998) 159.

[8] D.M. Liu, H.M. Chou, J.D. Wu, J. Mater. Sci. Mater. Med. 5 (1994) 147.

[9] J.I. Huaxia, C.B. Ponton, P.M. Marquis, J. Mater. Sci. Mater. Med. 3 (1992) 283.

[10] L.G. Ellies, D.G.A. Nelson, J.D.B. Featherstone, Biomaterials 13 (1992) 313.

[11] J.C. Elliott, Structure and Chemistry of the Apatites and Other Calcium Orthophosphates, Elsevier, Amsterdam, 1994.

[12] S. Downes, L. DiSilvio, C.P.A.T. Kleinand, M.V. Kayser, J. Mater. Sci. 2 (1991) 176.

[13] M. Otsuka, Y. Matsuda, T. Kokubo, S. Yashihara, T. Nakamura, T. Yamamuro, J. Biomed. Mater. Res. 29 (1995) 33.

[14] P.F. Kiser, G. Wilson, D. Needham, Nature 394 (1998) 459.

[15] H. Chaair, J.C. Heughebaert, M. Heughebaert, J. Mater. Chem. 5 (1995) 895.

[16] M. Jarcho, C.H. Bolen, M.B. Thomas, J. Bobick, J.F. Kay, R.H. Dormus, J. Mater. Sci. 11 (1976) 2027.

[17] K. Kandori, A. Yasukawa, T. Ishikawa, Chem. Mater. 7 (1995) 26.

[18] S. Puajindanetr, S.M. Best, W. Bonfield, Br. Ceramic Trans. 93 (1994) 96.

[19] Y. Osaka, Y. Miura, K. Takeuchi, M. Asada, K. Takahasi, J. Mater. Sci. Mater. Med. 2 (1991) 51.

[20] P. Conflant, C. Barthelemy, A.M. Goyot-Hermann, J.C. Guyot, A. Semmoud, S.T.P. Pharma Sci. 7 (1997) 282.

[21] F. Shijang, P. Renyun, Z. Qiyun, T. Shunying, Y. Huigen, Chin. J. Chem. Eng. 1 (1993) 38.

[22] S. Lazic, J. Cryst. Growth 147 (1995) 147.

[23] S. Lazic, J. Katanic-Popovic, S. Zec, N. Miljevic, J. Cryst. Growth 165 (1996) 124.

[24] W.G. Perdok, J. Christofferson, J. Arends, J. Cryst. Growth 80 (1987) 149.

[25] Powder Diffraction File-Inorganic Set 6-10, Joint Committee on Powder Diffraction Standards, Philadelphia, 1967.

[26] B.O. Fowler, Inorg. Chem. 13 (1974) 194.

[27] H. Füredi-Milhofer, V. Hlady, F.S. Baker, R.A. Beebe, N.W. Wikholm, J.S. Kittelberger, J. Colloid Interf. Sci. 70 (1979) 1.